Bioorganic & Medicinal Chemistry Letters 20 (2010) 1924–1927

Contents lists available at ScienceDirect

Bioorganic & Medicinal Chemistry Letters

journal homepage: www.elsevier.com/locate/bmcl

Structure-based design and synthesis of novel P2/P3 modified, non-peptidic β-secretase (BACE-1) inhibitors

Stephen Hanessian [a,*], Zhihui Shao [a], Claudia Betschart [b], Jean-Michel Rondeau [b], Ulf Neumann [b], Marina Tintelnot-Blomley [b]

[a] Department of Chemistry, Université de Montréal, C. P. 6128, Succ. Centre-Ville, Montréal, P.Q., Canada H3C 3J7
[b] Novartis Institutes for BioMedical Research, Novartis Pharma AG, PO Box, CH-4002 Basel, Switzerland

ARTICLE INFO

Article history:
Received 10 December 2009
Revised 22 January 2010
Accepted 27 January 2010
Available online 2 February 2010

Keywords:
Protease inhibitor
Peptidomimetic
Alzheimer's disease

ABSTRACT

Starting from peptidomimetic BACE-1 inhibitors, the P2 amino acid including the P2/P3 peptide bond was replaced by a rigid 3-aminomethyl cyclohexane carboxylic acid. Co-crystallization revealed an unexpected binding mode with the P3/P4 amide bond placed into the S3 pocket resulting in a new hydrogen bond interaction pattern. Further optimization based on this structure resulted in highly potent BACE-1 inhibitors with selectivity over BACE-2 and cathepsin D.

Genetic links point to an excess level of cerebral amyloid β peptide (Aβ) as a major culprit in the pathogenesis of Alzheimer's disease (AD). Aβ is generated by the sequential proteolytic action of two transmembrane proteins, β- and γ-secretase, which excise mainly the 40 and 42 amino acid Aβ fragments from the membrane bound β-amyloid precursor protein (APP). A misbalance between Aβ production and its clearance from the brain, and subsequent degradation leads to the aggregation of Aβ into oligomers and plaques.[1] Especially oligomeric forms, starting from the size of dimers, are believed to be the neurotoxic entities leading to neurodegeneration, synaptic loss, impaired neurotransmission, and finally cognitive decline.[2] Being responsible for the first endoproteolytic cleavage step in the generation of Aβ, the aspartyl protease β-secretase (BACE-1) is an attractive target when aiming at the reduction of Aβ. There are a number of recent reviews in the literature on recent progress in the development of BACE-1 inhibitors.[3] However, despite intensive efforts, it has been very challenging to find compounds which combine high potency and selectivity with good brain penetration. Therefore, few compounds have entered early-stage clinical trials so far.[4]

In previous papers, we have described some of our efforts in reducing the peptidic character of peptide-derived BACE-1 inhibitors. In particular, we aimed at reducing P-glycoprotein-mediated efflux, which limits brain exposure and is often observed with peptide-like compounds.

The removal of the P3/P4 amide segment followed by macrocyclization (Scheme 1) leading to compounds active in vivo has been described recently.[5] As known from the first X-ray structure of OM99-2, the heptapeptide-derived inhibitor with BACE-1,[6] and from previous hydroxyethylene transition-state inhibitors,[5a] the P2/P3 amide nitrogen is not involved in a direct hydrogen bond. It forms a water-mediated interaction and can be methylated without substantial reduction in activity in the enzyme assay. This amide bond is therefore a target for the introduction of non-peptidic features.

We report herein on a conceptually novel approach to the design of P2/P3 modified inhibitors of BACE-1, which also allows for a wide variation in the P3 site. Since the simple exchange of the amide bond by an alkyl chain was expected to introduce too much flexibility, some rigidification was considered necessary. To this end we envisaged the incorporation of a 3-aminomethyl cyclohexane carboxylic acid motif to replace the P2/P3 amide (Scheme 1). Carbocyclic and heterocyclic motifs have been previously incorporated in peptidomimetics as constrained P1′ BACE-1 inhibitors.[7]

In the present series, the conformationally pre-organized cyclohexane scaffold was intended to serve as a rigid linker between P1 and P3, which conserves the position of both the P3 side chain as well as the P3/P4 amide (Fig. 1). As illustrated in Table 1, the optimal filling of the S3 pocket in the original compound series enhances potency by two orders of magnitude going from methyl to *iso*-butyl (compounds **1–3**).

The lipophilic carbocycle is placed in S2, a position that is filled with a polar amino acid of the natural substrate. However, in line

* Corresponding author. Tel.: +514 343 6738; fax: +514 343 5728.
E-mail address: stephen.hanessian@umontreal.ca (S. Hanessian).

0960-894X/$ - see front matter © 2010 Elsevier Ltd. All rights reserved.
doi:10.1016/j.bmcl.2010.01.139

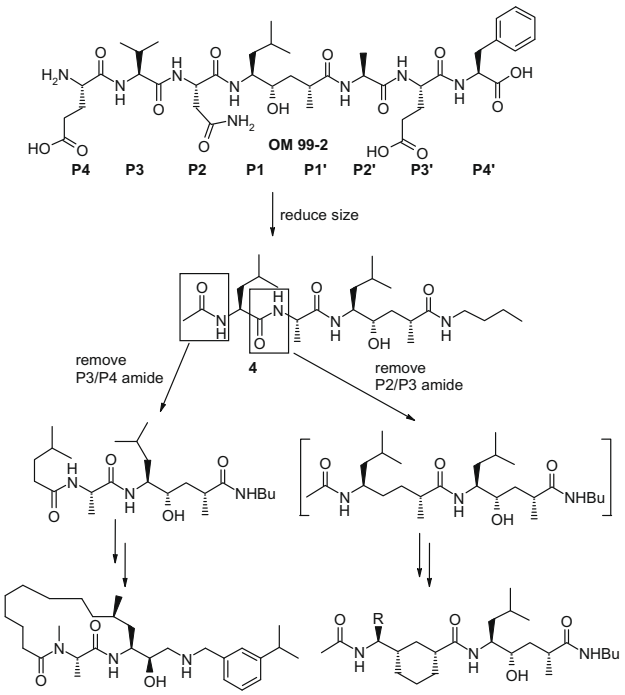

Scheme 1. Concepts for amide replacements to reduce peptidic character.

with the published subsite specificity of BACE-1,[9] the P2 amino acid can be replaced by methionine, and even alanine derivatives can lead to highly potent inhibitors (Table 1).

Initially, we prepared a series of P1 Phe hydroxyethylene isosteres with varying substituents at the P3 site (Table 2).[10]

In the previous peptidic series, activity convincingly increased from Me to *i*Bu with groups filling the S3 pocket more tightly (Table 1). This is in line with the co-crystal structure of compound **3** that shows the *i*Bu group filling the S3 pocket. Surprisingly, more bulky R_1 substituents (going from Me to Et, Pr, *i*Bu) at the novel aminomethyl cyclohexane scaffold were virtually devoid of activity (Table 2, compounds **5–7**, **9**). As an exception, the *i*Pr derivative **8** showed submicromolar activity on BACE-1, and the closely related enzymes BACE-2 and cathepsin D. Additionally, the dimethyl compound **10** and the cyclopentyl derivative **11** showed micromolar activity. Both observations were in contrast to the originally assumed position of this feature in the S3 pocket.

A co-crystal structure of the dimethyl compound **10** with BACE-1 explained the so far puzzling data.[11] As shown in Figure 2 the positions of the P3 alkyl and P3/P4 amide of compound **10** are

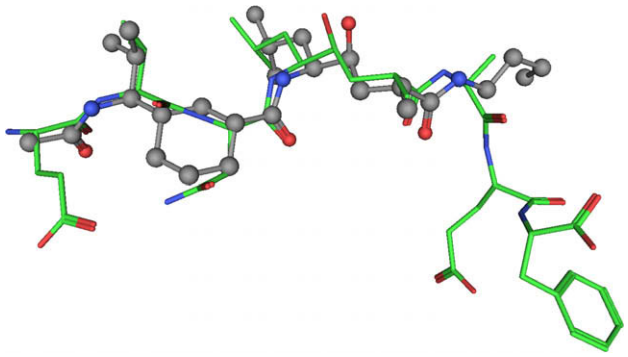

Figure 1. Modeled P2–P3 cyclohexyl analogue of compound **2** (ball-and-stick) in comparison to OM99-2 (stick), the ligand in the co-crystal structure used for calculations. Modeling and docking were done in the Flo modeling package.[8]

Table 1
P2/P3 SAR for some P3 to P2′ spanning hydroxyethylene compounds

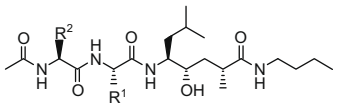

Compound	R^1	R^2	BACE-1	CathD
			IC_{50}[a], μM	
1	MeS–C_2H_4–	Me	4.0	0.035
2	MeS–C_2H_4–	iPr	0.37	0.048
3	MeS–C_2H_4–	iBu	0.053	0.009
4	Me	iBu	0.12	0.26

[a] Values are means of at least three experiments. IC_{50} values for human BACE-1 and human CathD inhibition were determined as described.[5a]

Table 2
SAR of P3 to P2′ spanning P2/P3 cyclohexyl hydroxyethylenes

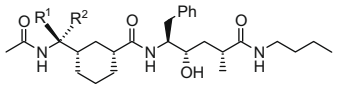

Compound	R^1	R^2	BACE-1	BACE-2	CathD
			IC_{50} (μM), or % inhib. at 10 μM		
5	Me	H	8%	14%	71%
6	Et	H	17%	24%	64%
7	Pr	H	15%	80%	84%
8	iPr	H	0.80	0.17	0.15
9	iBu	H	11%	42%	43%
10	Me	Me	3.7	0.37	0.24
11	–$(CH_2)_4$–		2.7	1.5	0.17

flipped in comparison to the canonical peptidic interaction pattern. In the binding pattern of peptides, or peptide mimics such as OM99-2 or compound **3**, there are two hydrogen bonds formed with Thr232 of BACE-1, one between the P2/P3 amide carbonyl and Thr232 NH, and an energetically less valuable one between the P3/P4 amide NH and the Thr232 hydroxyl group. A comparable orientation for compounds without a P2/P3 amide could only make use of the weaker ligand NH interaction whilst keeping its carbonyl unused. The binding pattern for compound **10** changed by flipping the P3/P4 amide into the S3 pocket, resulting in strong interactions of the amide carbonyl through hydrogen bonds with the Thr232 NH and Thr232 hydroxyl group.

With the structural information gleaned from the X-ray data, we sought to introduce functional and spatial elements in the P3 site that would improve the activity and selectivity. To circumvent stereochemical issues, we continued with symmetrically disubstituted gem-dimethyl derivatives of **10**.

Toward this objective, we prepared a series of N-acylated 3-(1-amino-1-methyl-ethyl)-cyclohexane carboxylic acids starting with the enantioenriched nitro intermediate **12** (Scheme 2).[12] Final compounds **26–28** were obtained from these building blocks and fragment **23** by standard coupling procedures (analogous to Scheme 3).

Modeling studies had also indicated that the S3 site could accommodate 5- and six-membered lactams. These were prepared as shown in Scheme 3.[12] Thus, the *N*-allyl intermediate **18** was acylated to **19** and **20**, respectively, then subjected to ring-closing metathesis in the presence of 5 mol % of Grubbs' first generation catalyst[13] to give the unsaturated lactams **21** and **22** in excellent yields. Catalytic hydrogenation and coupling with the amine fragment **23** afforded **24** and **25** in good yields after purification.

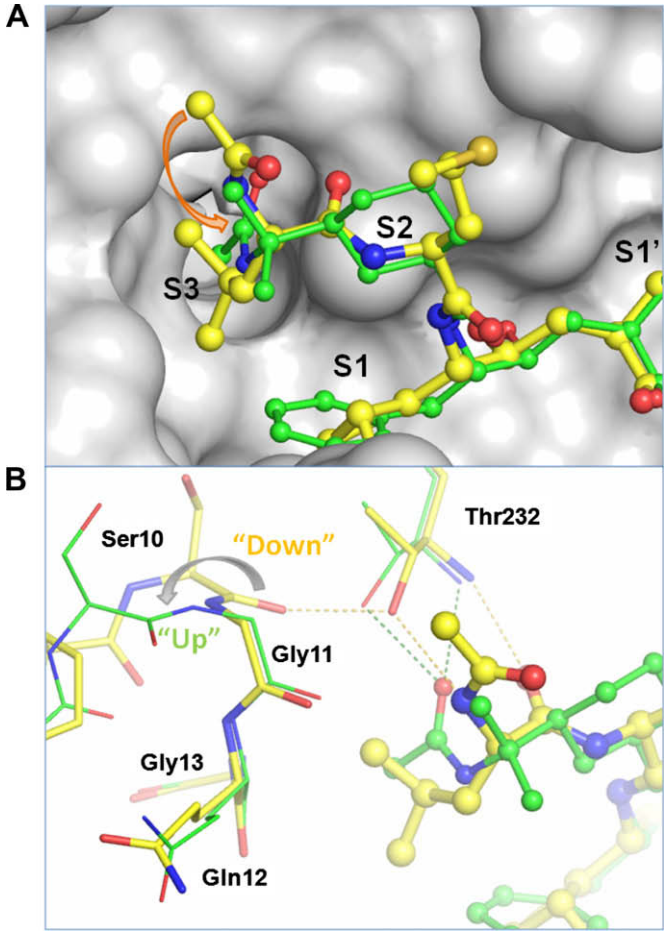

Figure 2. (A) Overlay of compound **3** (yellow) and compound **10** (green) co-crystal structures. (B) Hydrogen bonding to Thr232: Thr232 hydroxyl is an acceptor in the interaction with compound **3**, a donor in the interaction with compound **10**.

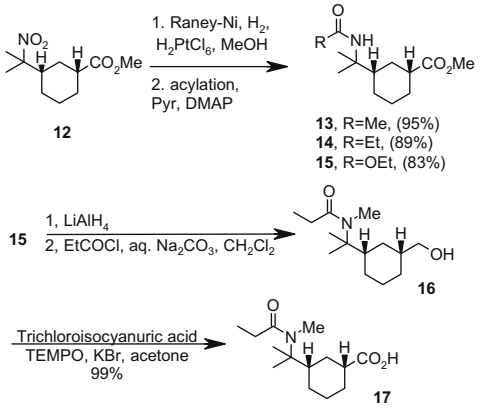

Scheme 2.

As previously reported,[5] a change of the transition-state mimetic moiety from hydroxyethylene (HE) to hydroxyethylamine (HEA) was done in anticipation of an improved in vitro as well as cellular activity. This benefit also materialized in this series (Table 3). Whilst in the HE-series small acyl variations (e.g., from methyl to ethyl) did not improve activity, small changes in the P3 site in the HEA series led to a breakthrough in activity (Table 3, compounds **26**–**28**). As seen in the co-crystal structure of compound **10** (Figs. 2A and B), the amide NH is not utilized for direct interactions with the protein, whilst there is additional room for tighter

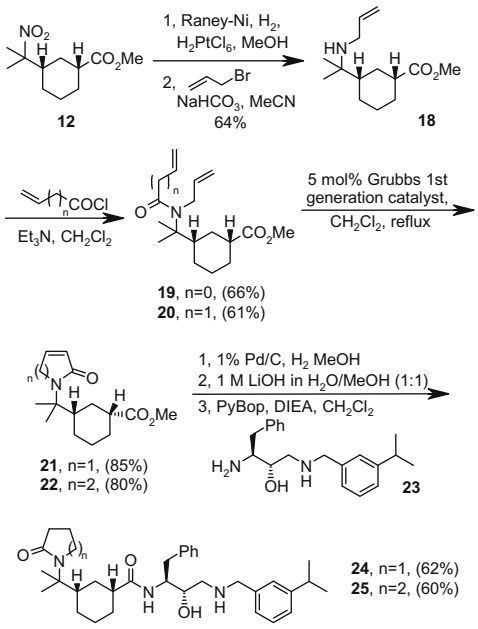

Scheme 3.

Table 3
SAR in P3 for P2/P3 cyclohexyl hydroxyethylamines

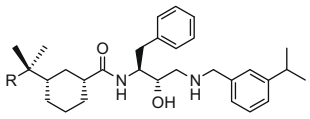

Compound	R	BACE-1 IC_{50}, μM	BACE-2	CathD	$A\beta_{40}$ CHO IC_{50}[a], μM
26		4.2	3.8	7.9	No data
27		0.58	3.7	7.1	No data
28		0.15	0.20	0.41	0.66
24		0.025	0.96	0.56	0.13
25		0.0025	0.14	0.12	0.067

[a] Inhibition of cellular release of $A\beta_{40}$ was determined as described.[5]

interactions in the S3 pocket. Consequently, amide alkylation as in compound **28**, results in improved activity (Table 3).

In this case, it is rather the balance of the different effects on the three related enzymes BACE-1, BACE-2, and CathD, which is most remarkable. An optimization for the tight fit in S3, especially by connecting the ethyl group with the *N*-methyl to form the lactam **24**, nearly exclusively improves BACE-1 activity, whilst the effects on BACE-2 and CathD stay comparably constant. It was predicted from the model, that the six-membered lactam **25** would fill the S3 pocket even better than the five-membered lactam **24**. Indeed, going from **24** to the homolog **25**, we again gained an order of magnitude in activity toward BACE-1. A co-crystal structure of compound **25** with BACE-1 confirmed the snug fit of the lactam in the S3 pocket[11] (Fig. 3). Intramolecular hydrophobic contacts

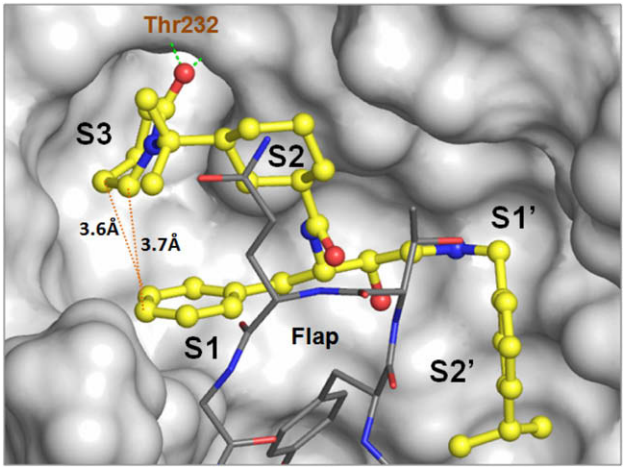

Figure 3. Compound **25** from co-crystal structure with BACE-1—interaction surface shown.

between the P3 lactam ring and the P1 phenyl may also contribute to the enhanced potency through pre-organization of the conformation of the active inhibitor.

The different effect on BACE-1 compared to CathD might be understood by comparing the S3 pockets of the two enzymes. Whilst there is a very tight fit towards the Ser10-Gly13 loop for compound **25** in BACE-1, this pocket (Ala13-Gln14), appears to be more open in CathD and BACE-2,[14] resulting in a less pronounced gain in activity by slightly larger acyl replacements. Moreover, two distinct conformations of the Ser10-Gly13 loop have been observed with BACE complexes.[15] While compound **3** binds to the 'down' conformation, compounds **10** and **25** select the 'up' conformation of the Ser10-Gly13 loop (see Fig. 2), thus achieving improved activity and selectivity. However, the size and shape of the extended S3 subpocket (S3sp)[15c] are not fulfilled with the P3 features in the above-described series of BACE-1 inhibitors.

In summary, starting from peptidomimetic BACE-1 inhibitors with counter selectivity for CathD, and going through several steps of optimization, we identified a highly potent, non-peptidic BACE-1 inhibitor with about 50-fold selectivity over BACE-2 and CathD and good cellular activity. As mentioned above, efflux by P-glycoprotein (located in the blood–brain barrier) often limits the brain exposure of BACE-1 inhibitors. Unfortunately, testing our most active compound **25** in the series in an in vitro model (MDCK cells stably transfected with the gene for the human P-glycoprotein transporter),[16] resulted in a high efflux ratio (BA/AB = 97). Thus, contrary to our initial expectations, the modification of the P2/P3 amide region exemplified by the low nanomolar prototype inhibitor **25**, did not overcome this challenging problem. Further efforts will be required to optimize and improve upon these results.

Acknowledgments

We thank the NSERC of Canada and Novartis (Basel, Switzerland) for generous financial assistance through the Medicinal Chemistry Chair program.

X-ray data collection was performed at the Swiss Light Source, Paul Scherrer Institut, Villigen, Switzerland, for the BACE complexes with compounds **3** and **10**. We are grateful to the machine and beamline groups whose outstanding efforts have made these experiments possible.

Supplementary data

Supplementary data associated with this article can be found, in the online version, at doi:10.1016/j.bmcl.2010.01.139.

References and notes

1. Crouch, P. J.; Harding, S.-M. E.; White, A. R.; Camakaris, J.; Bush, A. I.; Masters, C. L. *Int. J. Biochem. Cell Biol.* **2008**, *40*, 181.
2. Shankar, G. M.; Li, S.; Mehta, T. H.; Garcia-Munoz, A.; Shepardson, N. E.; Smith, I.; Brett, F. M.; Farrell, M. A.; Rowan, M. J.; Lemere, C. A.; Regan, C. M.; Walsh, D. M.; Sabatini, B. L.; Selkoe, D. J. *Nat. Med.* **2008**, *14*, 837.
3. For example, see: (a) Stachel, J. S. *Drug Dev. Res.* **2009**, *70*, 101; (b) Cole, S. L.; Vassar, R. *Curr. Alzheimer Res.* **2008**, *5*, 100; (c) Ghosh, A. K.; Kumaragurubaran, N.; Hong, L.; Koelsch, G.; Tang, J. *Curr. Alzheimer Res.* **2008**, *5*, 12; (d) Hills, I. D.; Vacca, J. P. *Curr. Opin. Drug Discov. Devel.* **2007**, *10*, 383; (e) Durham, T. B.; Shepherd, T. A. *Curr. Opin. Drug Discov. Devel.* **2006**, *9*, 7761.
4. For example, see: (a) Ghosh, A. K.; Gemma, S.; Tang, J. *Neurotherapeutics* **2009**, *5*, 399; (b) Rafii, M. S.; Aisen, P. S. *BMC Med.* **2009**, *7*, 7.
5. (a) Machauer, R.; Veenstra, S.; Rondeau, J.-M.; Tintelnot-Blomley, M.; Betschart, C.; Neumann, U.; Paganetti, P. *Bioorg. Med. Chem. Lett.* **2009**, *19*, 1361; (b) Machauer, R.; Laumen, K.; Veenstra, S.; Rondeau, J.-M.; Tintelnot-Blomley, M.; Betschart, C.; Jaton, A.-L.; Desrayaud, S.; Staufenbiel, M.; Rabe, S.; Paganetti, P.; Neumann, U. *Bioorg. Med. Chem. Lett.* **2009**, *19*, 1366.
6. PDB ID: 1FKN; (a) Hong, L.; Koelsch, G.; Lin, X.; Wu, S.; Terzyan, S.; Gosh, A. K.; Zhang, X. C.; Tang, J. *Science* **2000**, *290*, 150; (b) Ghosh, A. K.; Bilcer, G.; Harwood, C.; Kawahama, R.; Shin, D.; Hussain, K. A.; Hong, L.; Loy, J. A.; Nguyen, C.; Koelsch, G.; Ermolieff, J.; Tang, J. *J. Med. Chem.* **2001**, *44*, 2865.
7. (a) Hanessian, S.; Yun, H.; Hou, Y.; Yang, G.; Bayrakdarian, M.; Therrien, E.; Moitessier, N.; Roggo, S.; Veenstra, S.; Tintelnot-Blomley, M.; Rondeau, J.-M.; Ostermeier, C.; Strauss, A.; Ramage, P.; Paganetti, P.; Neumann, U.; Betschart, C. *J. Med. Chem.* **2005**, *48*, 5175; (b) Hanessian, S.; Yun, H.; Hou, Y.; Tintelnot-Blomley, M. *J. Org. Chem.* **2005**, *70*, 6735; (c) Hanessian, S.; Hou, Y.; Bayrakdarian, M.; Tintelnot-Blomley, M. *J. Org. Chem.* **2005**, *70*, 6746.
8. McMartin, C.; Bohacek, R. S. *J. Comput. Aided. Mol. Des.* **1997**, *11*, 333.
9. Turner, R. T., III; Koelsch, G.; Hong, L.; Castanheira, P.; Gosh, A.; Tang, J. *Biochemistry* **2001**, *40*, 10001.
10. Details of the synthesis will be published elsewhere. See also Supplementary data.
11. X-ray coordinates for the complex of BACE-1 with inhibitors **3**, **10**, and **25** have been deposited in the Protein Data Bank (http://www.rcsb.org), and can be accessed under PDB ID: 3K5D, 3K5F, and 3K5G.
12. See Supplementary data for full experimental details.
13. Schwab, P.; France, M. B.; Ziller, J. W.; Grubbs, R. H. *Angew. Chem., Int. Ed.* **1995**, *34*, 2039.
14. (a) CathD: unpublished data.; BACE-2: PDB ID: 2EWY; (b) Ostermann, N.; Eder, J.; Eidhoff, U.; Zink, F.; Hassiepen, U.; Worpenberg, S.; Maibaum, J.; Simic, O.; Hommel, U.; Gerhartz, B. *J. Mol. Biol.* **2006**, *355*, 249.
15. (a) Stauffer, S. R.; Stanton, M. G.; Gregro, A. R.; Steinbeiser, M. A.; Shaffer, J. R.; Nantermet, P. G.; Barrow, J. C.; Rittle, K. E.; Collusi, D.; Espeseth, A. S.; Lai, M.-T.; Pietrak, B. L.; Holloway, M. K.; McGaughey, G. B.; Munshi, S. K.; Hochman, J. H.; Simon, A. J.; Selnick, H. G.; Graham, S. L.; Vacca, J. P. *Bioorg. Med. Chem. Lett.* **2007**, *17*, 1788; (b) McGaughey, G. B.; Colussi, D.; Graham, S. L.; Lai, M.-T.; Munshi, S. K.; Nantermet, P. G.; Pietrak, B.; Rajapakse, H. A.; Selnick, H. G.; Stauffer, S. R.; Holloway, M. K. *Bioorg. Med. Chem. Lett.* **2007**, *17*, 1117; (c) Coburn, C. A.; Stachel, S. J.; Li, Y.-M.; Rush, D. M.; Steele, T. G.; Chen-Dodson, E.; Holloway, M. K.; Xu, M.; Huang, Q.; Lai, M.-T.; DiMuzio, J.; Crouthamel, M.-C.; Shi, X.-P.; Sardana, V.; Chen, Z.; Munshi, S.; Kuo, L.; Makara, G. M.; Annis, D. A.; Tadikonda, P. K.; Nash, H. W.; Vacca, J. P.; Wang, T. *J. Med. Chem.* **2004**, *47*, 6117.
16. Wang, Q.; Rager, J. D.; Weinstein, K.; Kardos, P. S.; Dobson, G. L.; Li, J.; Hidalgo, I. J. *Int. J. Pharm.* **2005**, *288*, 349.